VIP Materials Synthesis

DOI: 10.1002/ange.201206203

"Hard–Soft" Synthesis of $SrCrO_{3-\delta}$ Superstructure Phases**

*Angel M. Arévalo-López, Jennifer A. Rodgers, Mark S. Senn, Falak Sher, James Farnham, William Gibbs, and J. Paul Attfield**

"Soft" reactions, which alter local chemistry and structure while retaining the basic lattice arrangement, are important for synthesizing solids with novel properties.[1,2] For example, new layered oxides $LaNiO_2$ and $SrFeO_2$ were prepared by reduction of the corresponding perovskites at temperatures as low as 190 °C.[3,4] Precursors for "soft" chemistry are usually prepared at ambient pressure and sometimes under moderate gas pressures, for example, 10–30 MPa of oxygen gas was used to produce fully oxidized $LaNiO_3$ and $SrFeO_3$ perovskites for the latter reactions. "Hard" high-pressure (1–20 GPa) conditions can lock instabilities, such as unusual oxidation states or coordination environments, into dense phases that are metastable when recovered to ambient conditions, thus leading to unusual properties, such as intermetallic charge transfer and negative thermal expansion in $LaCu_3Fe_4O_{12}$ and $BiNiO_3$.[5,6] Hence, it is attractive to explore combined "hard–soft" routes[7] to novel materials by partially relieving the instability of a high-pressure precursor through post-synthesis modification.

We have explored "hard–soft" oxide chemistry by investigating the reduction of $SrCrO_3$. Cr^{4+} usually has tetrahedral coordination in oxides prepared at ambient pressure, and high pressures are needed to generate octahedral environments, for example, when Sr_2CrO_4 is compressed from the ambient K_2SO_4-type to the denser K_2NiF_4-type polymorph.[8] Pressures higher than 4 GPa are needed to synthesize $SrCrO_3$, which adopts the cubic perovskite structure with Cr^{4+} in octahedral coordination.[9,10,11] $SrCrO_3$ thus offers the possibility for transforming $Cr^{4+}O_6$ octahedra to $Cr^{4+}O_4$ tetrahedra at low temperatures, while preserving the underlying perovskite arrangement, thus generating new structures through a "hard–soft" route.

Polycrystalline $SrCrO_3$ samples were synthesized by a high-pressure technique and reduced by heating in flowing hydrogen gas or in sealed evacuated tubes with calcium hydride (experimental details and additional Tables S1 and S2 and Figures S1–S4 are shown in Supporting Information).

[*] Dr. A. M. Arévalo-López, Dr. J. A. Rodgers, M. S. Senn, Dr. F. Sher, J. Farnham, W. Gibbs, Prof. J. P. Attfield
Centre for Science at Extreme Conditions (CSEC) and School of Chemistry, University of Edinburgh
Mayfield Road, Edinburgh EH9 3JZ (UK)
E-mail: j.p.attfield@ed.ac.uk
Dr. F. Sher
School of Science and Engineering
Lahore University of Management Sciences (LUMS) (Pakistan)

[**] We acknowledge support from the EPSRC, STFC, the Leverhulme Trust, the Royal Societies of Edinburgh and London, and LUMS.

Supporting information for this article is available on the WWW under http://dx.doi.org/10.1002/anie.201206203.

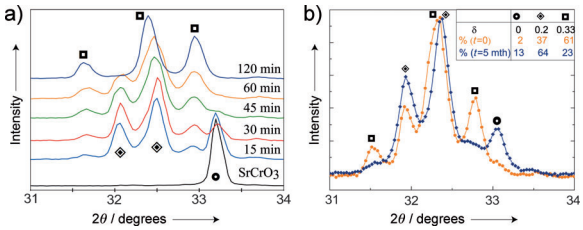

Figure 1. Powder X-ray diffraction data for a) the progressive reduction of $SrCrO_3$ at 450 °C under an atmosphere of 95 % Ar and 5 % H_2, and b) a reduced-$SrCrO_3$ sample before and after standing in a sealed vial under air for five months. Inset: fitted phase fractions, showing the $\delta = 0.25 \rightarrow 0.2 \rightarrow 0$ re-oxidation. Circles/diamonds/squares correspond to peaks from $\delta = 0/0.2/0.25$ phases, respectively.

Powder X-ray diffraction showed that two crystalline $SrCrO_{3-\delta}$ products were formed between 400 and 500 °C (Figure 1), both with complex diffraction patterns related to that of the cubic precursor. It proved very difficult to isolate single-phase samples of these two new compounds because of their similar compositions and facile re-oxidation to $SrCrO_3$. However, both crystal structures were determined from powder diffraction patterns of mixed $\delta = 0/0.2/0.25$ phase samples, as described below. The $\delta = 0.25$ composition of the final phase was determined by thermogravimetry (Figure S1) and confirmed by the crystal structure. No thermogravimetric plateau was observed for the intermediate phase and the $\delta = 0.2$ composition was deduced from the structural analysis. Attempts to prepare the $SrCrO_{3-\delta}$ phases without use of the high-pressure $SrCrO_3$ precursor (such as by reduction of the ambient-pressure compound $SrCrO_4$) were unsuccessful, thus confirming that they are products of topochemical reactions.

A slow re-oxidation of both $SrCrO_{3-\delta}$ phases to $SrCrO_3$ was observed at room temperature on exposure to small amounts of air (Figure 1b). This is a notable observation, because Cr^{3+}-containing oxides are not usually oxidized by ambient air. The regenerated $SrCrO_3$ samples were as highly crystalline as the original precursors (see Figure S1), thus showing that the structural changes are fully reversible and that these perovskites have appreciable oxide ion mobility at room temperatures. The $SrCrO_{3-\delta}$ phases were rapidly re-oxidized to $SrCrO_3$ on heating, for example, in less than one hour in air at 250 °C.

X-ray diffraction peaks from the initial reduced-$SrCrO_3$ phase were indexed on a rhombohedral (R) unit cell with a long (34.5 Å) c-axis. This observation evidences a repeat sequence of 15 close-packed SrO_3 layers stacked perpendicular to the [111] (body-diagonal) direction of the cubic perovskite structure. 15R-perovskites with mixed cubic (*c*)

and hexagonal (*h*) stacking sequences $(chchc)_3$ (e.g., $SrMn_{1-x}Fe_xO_{3-\delta}$)[12] or $(hhchh)_3$ (e.g., $BaMnO_3$)[13] have the same cell symmetry, but these models did not fit the diffraction intensities. Instead, the $SrCrO_{3-\delta}$ phase was found to be isostructural with the complex oxide $Ba_5MnNa_2V_2O_{13}$,[14] with Sr at the Ba sites and Cr at the Mn, Na, and V positions. The full structure was refined by using powder X-ray and neutron diffraction profiles (Figure 2 and Table S1). $Ba_5MnNa_2V_2O_{13}$ has partly disordered vacancies, but all sites in the $SrCrO_{3-\delta}$ phase were found to be fully occupied, corresponding to the $\delta = 0.2$ composition $SrCrO_{2.8}$ ($Sr_5Cr_5O_{14}$). The $Ba_5MnNa_2V_2O_{13}$ structure has not been reported in simpler materials, so $SrCrO_{2.8}$ represents a new ternary aristotype for perovskite-related structures.

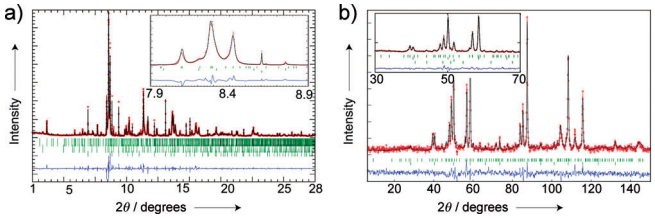

Figure 2. a) Synchrotron X-ray profile for a reduced-$SrCrO_3$ sample of 72% $SrCrO_{2.8}$, 16% $SrCrO_3$, and 8% Cr_2O_3 by mass. b) Neutron data for a sample containing 43% $SrCrO_{2.8}$ and 57% $SrCrO_3$. Insets: $SrCrO_{2.8}$ peak splittings. Phase markers are shown in order from top to bottom. The model for $SrCrO_{2.8}$ was simultaneously refined in fits (a) and (b).

The crystal structure of $SrCrO_{2.8}$ ($Sr_5Cr_5O_{14}$) consists of stacked cubic perovskite layers in a $(ccc'cc)_3$ sequence (Figure 3a). One oxide is lost from every fifth (c') SrO_3 layer, and the remaining two undergo an elegant rearrangement, becoming coordinated to one Cr, and thus create tetrahedral environments in the two adjacent Cr layers. The other three Cr layers retain the octahedral coordination of the parent perovskite structure. Bond valence sum (BVS)[15] estimates of the oxidation states of the three distinct Cr sites (Table S1) show that tetrahedral sites contain Cr^{4+}, while the two octahedral sites have $Cr^{3.5+}$ and Cr^{3+} states. The sequence of Cr layers gives rise to a charge-density wave-type order (Figure 3a).

Reduction and rearrangement of $SrCrO_3$ to form $SrCrO_{2.8}$ is very efficient in the generation of favorable coordination environments for the Cr ions. These environments reflect ionic sizes and ligand field stabilization energies; Cr^{4+} is a small $3d^2$ ion that tends to occupy tetrahedral sites in ambient-pressure oxides, while $3d^3$ Cr^{3+} usually has octahedral coordination. All Cr^{4+} are octahedrally coordinated in $SrCrO_3$, but reconstruction of only 12% of the total atoms (through loss or displacement of the anions in every fifth close-packed layer) gives $SrCrO_{2.8}$ ($Sr_5Cr_5O_{14}$), in which 4/5 of the Cr ions are in favorable environments (two tetrahedral Cr^{4+} and two octahedral Cr^{3+}), and only 1/5 of the original Cr^{4+} ions remain octahedrally coordinated.

X-ray diffraction peaks from the final reduction product $SrCrO_{2.75}$ ($Sr_4Cr_4O_{11}$) were indexed on a primitive monoclinic cell, showing a distorted stacking of six cubic close-packed layers perpendicular to the cubic [111] direction. A good fit to the diffraction data was obtained using the model shown in Figure 3b, which has a $c'ccccc$ stacking sequence (refinement results are given in Figure S2 and Table S2) Half of the original oxide anions are lost from the c' $SrO_{1.5}$ layers, one-third are displaced to new sites such as those in $SrCrO_{2.8}$, and one-sixth retain their close-packed positions. This again creates a double tetrahedral layer, but half of the tetrahedra are distorted and share corners, thus breaking the threefold symmetry. This results in a monoclinic structure of alternating slabs of double-tetrahedral and quadruple-octahedral layers.

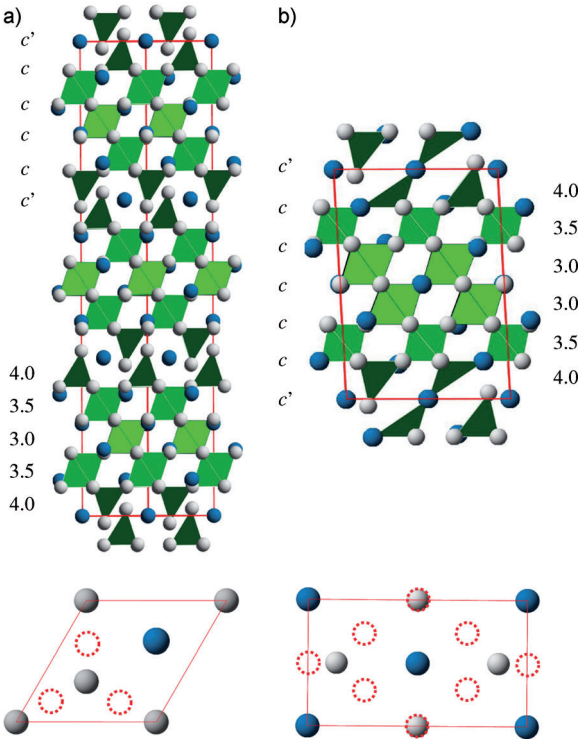

Figure 3. a) 15-layer rhombohedral structure of $SrCrO_{2.8}$. b) Monoclinically distorted 6H-structure of $SrCrO_{2.75}$. The layer-stacking (z-axis) directions are vertical in the upper diagrams and the repeat sequences of cubic perovskite-type (*c*) and reconstructed (*c'*) planes are shown. Charge-density wave-type variations of the formal Cr states are labeled and illustrated by the dark/medium/light green of the $Cr^{4+}O_4/Cr^{3.5+}O_6/Cr^{3+}O_6$ polyhedra. (001) views of the reconstructed *c'* layers are shown below each structure, with Sr (blue) and O (gray) atoms, and oxide positions in the original close-packed SrO_3 layer as broken red circles.

The distorted six-hexagonal layer (6H)-perovskite $SrCrO_{2.75}$ model is a new structure type. Unconstrained refinement of all atomic coordinates in this complex monoclinic structure was not possible, so reliable BVS estimates of Cr states are unavailable. The proposed charge distribution in Figure 3b is assigned by analogy with that of $SrCrO_{2.8}$. Tetrahedral sites host Cr^{4+}, the adjacent octahedral layers contain average $Cr^{3.5+}$ states, and the two central layers host Cr^{3+}. This again describes a charge-density wave-type distribution driven by ligand field effects. Reconstruction of only 8.3% of the atoms in $SrCrO_3$ to give $SrCrO_{2.75}$ is highly efficient in placing 5/6 of the Cr ions (two tetrahedral Cr^{4+} and three octahedral Cr^{3+}) in favorable coordination environments.

Vacancies in $SrCrO_{3-\delta}$ ($\delta = 0.2$ and 0.25) are formed in (111)-type c' planes, in contrast to other reduced $ABO_{3-\delta}$ perovskites, in which the deficient layers are usually parallel to cubic (100) planes. The reconstructed c' layers in both $SrCrO_{3-\delta}$ phases generate only tetrahedral coordination of the adjacent Cr cations. In contrast, the lowest B-cation coordination initially decreases from six to five (square-pyramidal) for comparable δ values (≈ 0.20–0.25) in other systems, such as $CaMnO_{3-\delta}$ ($0.2 \le \delta \le 0.5$). At higher δ values, such as in the $ABO_{2.5}$ brownmillerite structure, four coordination is observed. The $SrCrO_{3-\delta}$ structures are also unusual because oxide vacancies are segregated into widely (five- or six-layer) spaced (111) planes with close-packed slabs of native perovskite in-between (Figure 3), whereas defects in conventional reduced perovskites occur in a high proportion of the planes, for example, every second BO_2 (100) layer in brownmillerites. The $SrCrO_{3-\delta}$ mechanism gives rise to large-scale superstructures of the cubic perovskite structure; the 34.5 Å c-axis of $SrCrO_{2.8}$ is almost an order of magnitude higher than the 3.8 Å cell parameter of the precursor. Long periodicities due to mixed *c/h* layer stackings are well-known in hexagonal perovskites prepared at high temperatures, such as the 15R materials $SrMn_{1-x}Fe_xO_{3-\delta}$ and $BaMnO_3$.[12,13] However, the emergence of such large-scale structures from low-temperature reduction of a simple cubic perovskite is unprecedented.

Chromium oxide perovskites, such as $(La_{1-x}Sr_x)CrO_{3-\delta}$ and $(La_{1-x}Sr_x)(Cr_{1-y}M_y)O_{3-\delta}$ (M = Mn, Fe, Co, Ni) derivatives, have mixed (electronic and ionic) conductivity from variable Cr^{3+}/Cr^{4+} valences and oxide vacancies, and are used in solid-oxide fuel cell (SOFC) anodes.[16] Hence, anion- and charge-ordered $SrCrO_{2.75}$ and $SrCrO_{2.8}$ may be relevant model compounds. Although these phases are not stable under high-temperature and low-oxygen partial pressure SOFC anode environments, we have discovered that the $SrCrO_{2.8}$-type superstructure is stabilized in $Sr(Cr_{1-x}Fe_x)O_{3-y}$ ($0.4 < x < 0.6$), which is synthesized at such conditions without the use of high pressure (see Figure S3). This type of structure was not identified in previous work;[17] full results on $Sr(Cr_{1-x}Fe_x)O_{3-y}$ will be published separately. Oxide diffusion rates are maximal in the vacancy-containing (100) planes of $CaFeO_{2.5}$ brownmillerite,[18] thus diffusion may be most rapid within deficient (111) c' layers in $SrCrO_{3-\delta}$ and other reduced Cr perovskites.

Structural changes that accompany the reduction of $SrCrO_3$ appear principally to relieve the local coordination instability of Cr^{4+}. However, the long-period structural modulations may also have an electronic component. The $\delta = 0.2$ and 0.25 $SrCrO_{3-\delta}$ superstructures are similar, but they do not belong to a simple homologous series. The $\delta = 0.2$ structure loses a third of the oxide ions from one in every $(1/\delta) = 5$ close-packed SrO_3 layers. The same mechanism predicts a four-layer repeat for $\delta = 0.25$, and this appears perfect for relaxing local coordination environments as it would generate two tetrahedral Cr^{4+} and two octahedral Cr^{3+} layers. However, the $\delta = 0.25$ structure has half the oxide ions missing from every sixth SrO_3 layer, consistent with Cr^{3+}-$Cr^{3.5+}$-Cr^{4+} charge modulation, such as that observed in the $\delta = 0.2$ structure (see Figure 3), whereas the alternative four-layer $\delta = 0.25$ structure would have adjacent Cr^{3+} and Cr^{4+} planes. Thus, it appears that long-period Cr charge-density waves are also important to the stabilization of the two $SrCrO_{3-\delta}$ superstructures, and these result in mixed-valent $Cr^{3.5+}$ layers between tetrahedral Cr^{4+} and octahedral Cr^{3+} planes.

Although phase-pure samples of $SrCrO_{3-\delta}$ ($\delta = 0.2$ and 0.25) were not obtained, their essential magnetic properties were determined by susceptibility measurements in a 0.5 T field (Figure 4a). $SrCrO_3$ orders antiferromagnetically below

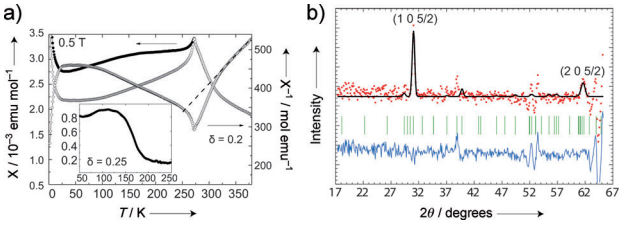

Figure 4. a) FC/ZFC magnetic susceptibilities (as filled/open circles) for $SrCrO_{2.8}$ and inverse ZFC data with a Curie–Weiss fit to 330–380 K points, giving a paramagnetic moment of 2.36 μ_B per Cr and a 25 K Weiss temperature. Inset: corrected FC susceptibility for $SrCrO_{2.75}$. b) Difference between $SrCrO_{2.8}$ neutron diffraction profiles at 200 and 300 K (Figure 2b), showing two magnetic ($h\ 0\ l+{}^1/_2$) diffraction peaks fitted by the model described in the text; other features are from thermal expansion shifts in nuclear peaks.

70 K, but the two $SrCrO_{3-\delta}$ phases show ordering features at much higher temperatures. $SrCrO_{2.8}$ has a sharp transition at $T_C = 272$ K, and the divergence of zero-field-cooled (ZFC) and field-cooled (FC) susceptibilities indicates that weak ferromagnetism or ferrimagnetic order is present. A positive Weiss temperature and deviations from Curie–Weiss behavior above T_C evidence strong ferromagnetic interactions. The estimated $SrCrO_{2.75}$ susceptibility, corrected by subtracting a $SrCrO_{2.8}$ contribution, has a broad maximum at approximately 100 K, which is consistent with short-range spin order in the triangular layers.

Long-range spin order in $SrCrO_{2.8}$ is confirmed by the appearance of two weak ($h\ 0\ l+{}^1/_2$) magnetic neutron diffraction peaks on cooling from 300 to 200 K (Figure 4b). Their intensities are fitted by a simple model (Figure S4), in which Cr spins in every layer are parallel, and each ferromagnetic layer is antiferromagnetically coupled to adjacent spin planes. Magnetic moments are parallel to the c-axis with refined magnitudes of 2.4(5), 1.3(3), and 1.1(2) μ_B for Cr^{3+}, $Cr^{3.5+}$, and Cr^{4+} layers, respectively. These values are consistent with ideal spin-only values of 3, 2.5, and 2 μ_B, after zero-point and covalent reductions of the moments, and demonstrate that the Cr charge-density wave (Figure 3a) gives rise to a spin-density wave-type modulation of magnetic moments with a long, doubled c-axis, periodicity ($2c \approx 69$ Å). The observed weak ferromagnetism may result from canting of the moments or short-range Cr^{3+}/Cr^{4+} charge and spin order in the mixed-valent planes, but the neutron data were not sensitive to these possibilities.

The discovery of $SrCrO_{2.75}$ and $SrCrO_{2.8}$ through low-temperature reduction of the precursor $SrCrO_3$ demonstrates

"hard–soft" transition-metal-oxide synthesis. Other than $SrCrO_3$, the only previously reported Sr-Cr-O phases with Sr:Cr ≈ 1:1 are $SrCrO_4$ and the misfit-layer compound $[Sr_2O_2][CrO_2]_{1.85}$[19], which are not structurally related to the $SrCrO_{3-\delta}$ phases. Many materials can be quenched from "hard" high-pressure conditions[20] (more than 60 new high-pressure perovskite oxides were reported in a recent review)[21] for subsequent exploration of "soft" modifications, such as reduction, oxidation, or intercalation reactions; thus, many new materials may be accessible through "hard–soft" chemistry. Availability of high-pressure precursors is a practical consideration, and the stability window for products between the onsets of reaction and decomposition of the metastable precursor may also be limiting; a 400–500 °C window was found for $SrCrO_{3-\delta}$ phases.

In conclusion, this study has demonstrated "hard–soft" oxide synthesis through low-temperature reduction of the high-pressure perovskite $SrCrO_3$ which gives two new $SrCrO_{3-\delta}$ phases ($\delta = 0.2$ and 0.25) with unusual superstructures and properties. Both are re-oxidized to cubic $SrCrO_3$ on standing in air, whereas Cr^{3+}-containing oxides are usually inert under these conditions. Cr^{4+} coordination is relaxed from octahedral geometry to the tetrahedral environment normally observed at ambient pressure through reconstruction of widely spaced (111) planes and formation of long-period Cr^{3+}/Cr^{4+} charge-density waves. The $SrCrO_{3-\delta}$ vacancy mechanism may be relevant to related SOFC anode materials; a discovered stabilization of the $\delta = 0.2$ superstructure by Fe substitution at ambient pressure supports this idea. Similar "soft" chemical modifications of "hard" high-pressure precursors that feature local instabilities may enable the discovery of further new materials and structural mechanisms.

Received: August 2, 2012
Published online: September 26, 2012

Keywords: high-pressure chemistry · oxides · perovskite phases · "soft" chemistry · vacancy ordering

[1] J. Gopalakrishnan, *Chem. Mater.* **1995**, *7*, 1265 – 1275.
[2] R. E. Schaak, T. E. Mallouk, *Chem. Mater.* **2002**, *14*, 1455 – 1471.
[3] M. A. Hayward, M. A. Green, M. J. Rosseinsky, J. Sloan, *J. Am. Chem. Soc.* **1999**, *121*, 8843 – 8854.
[4] Y. Tsujimoto, C. Tassel, N. Hayashi, T. Watanabe, H. Kageyama, K. Yoshimura, M. Takano, M. Ceretti, C. Ritter, W. Paulus, *Nature* **2007**, *450*, 1062 – 1065.
[5] Y. W. Long, N. Hayashi, T. Saito, M. Azuma, S. Muranaka, Y. Shimakawa, *Nature* **2009**, *458*, 60 – 63.
[6] M. Azuma, W. Chen, H. Seki, M. Czapski, S. Olga, K. Oka, M. Mizumaki, T. Watanuki, N. Ishimatsu, N. Kawamura, S. Ishiwata, M. G. Tucker, Y. Shimakawa, J. P. Attfield, *Nat. Commun.* **2011**, *2*, 347.
[7] P. F. McMillan, W. T. Petuskey, C. A. Angell, J. R. Holloway, G. H. Wolf, M. O. O'Keeffe, O. Sankey, *Mater. Sci. Forum* **1994**, *152 – 153*, 371 – 374.
[8] J. A. Kafalas, J. M. Longo, *J. Solid State Chem.* **1972**, *4*, 55 – 59.
[9] A. J. Williams, A. Gillies, J. P. Attfield, G. Heymann, H. Huppertz, M. J. Martínez-Lopez, J. A. Alonso, *Phys. Rev. B* **2006**, *73*, 104409.
[10] L. Ortega-San-Martin, A. J. Williams, J. Rodgers, J. P. Attfield, G. Heymann, J. Huppertz, *Phys. Rev. Lett.* **2007**, *99*, 255701.
[11] E. Castillo-Martínez, A. Durán, M. A. Alario-Franco, *J. Solid State Chem.* **2008**, *181*, 895 – 904.
[12] E. J. Cussen, J. Sloan, J. F. Vente, P. D. Battle, T. Gibb, *Inorg. Chem.* **1998**, *37*, 6071 – 6077.
[13] J. J. Adkin, M. A. Hayward, *Chem. Mater.* **2007**, *19*, 755 – 762.
[14] A. Bendraoua, E. Quarez, F. Abraham, O. Mentre, *J. Solid State Chem.* **2004**, *177*, 1416 – 1424.
[15] N. E. Brese, M. O'Keeffe, *Acta Crystallogr. Sect. B* **1991**, *47*, 192 – 197.
[16] P. I. Cowin, C. T. G. Petit, R. Lan, J. T. S. Irvine, S. Tao, *Adv. Energy Mater.* **2011**, *1*, 314 – 332.
[17] T. C. Gibb, M. Matsuo, *J. Solid State Chem.* **1990**, *86*, 164 – 174.
[18] S. Inoue, M. Kawai, N. Ichikawa, H. Kageyama, W. Paulus, Y. Shimakawa, *Nat. Chem.* **2010**, *2*, 213 – 217.
[19] E. Castillo-Martínez, A. M. Arévalo-López, R. Ruiz-Bustos, M. A. Alario-Franco, *Inorg. Chem.* **2008**, *47*, 8526 – 8542.
[20] P. F. McMillan, *Chem. Soc. Rev.* **2006**, *35*, 855 – 857.
[21] J. A. Rodgers, A. J. Williams, J. P. Attfield, *Z. Naturforsch. B* **2006**, *61*, 1515 – 1526.

